Research Square

Preprints are preliminary reports that have not undergone peer review.
They should not be considered conclusive, used to inform clinical practice,
or referenced by the media as validated information.

Candida albicans forms azole-resistant liquid-suspension biofilms with distinct characteristics and a potential to aid in dispersal

Françios A.B. Olivier
Monash University
Jaimee L. Renshaw
Monash University
Calvin Kraupner-Taylor
Monash University
Angavai Swaminathan
Monash University
Paul F. Harrison
Monash University
Traude H. Beilharz
Monash University
Ana Traven
ana.traven@monash.edu

Monash University

Article

Keywords:

Posted Date: October 20th, 2026

DOI: https://doi.org/10.21203/rs.3.rs-11227287/v1

License: This work is licensed under a Creative Commons Attribution 4.0 International License.
Read Full License

Additional Declarations: No competing interests reported.

Abstract

Candida albicans is a WHO "*critical priority*" human fungal pathogen for which biofilm formation on the surface of medical devices is associated with bloodstream infections and antifungal drug resistance. Our understanding of *C. albicans* biofilms is based primarily on studies of surface-adhered biofilms, while the full spectrum of biofilm morphologies that *C. albicans* may use to persist in the host remains underexplored. Here we show that *C. albicans* forms liquid-suspension biofilms when faced with a poorly adherent surface, or following prolonged maturation of surface-adhered biofilms which exhausts available surface for attachment. *C. albicans* liquid-suspension biofilms are resistant to the front-line antifungal drug fluconazole and display a complex structure consisting of dense clusters of heterogeneous cell morphologies (hyphal, pseudohyphal and yeast cells) connected to one another through extensive hyphal networks. Liquid-suspension biofilms share transcriptional programs with surface-adhered biofilms and are controlled by the same set of master transcriptional regulators. The transcriptomic profiles of liquid-suspension and surface-adhered biofilms converge over time. Moreover, after transfer to plastic surfaces, liquid-suspension biofilms can seed new surface-adhered biofilm growth. Our study characterises a previously unappreciated suspension biofilm morphology of *C. albicans*, shows that this is a *bona fide* drug-resistant biofilm with regulatory properties shared with canonical surface-adhered biofilms, and demonstrates that *C. albicans* transitions between surface-adhered and liquid-suspension biofilms depending on surface availability. Our findings establish *C. albicans* liquid-suspension biofilms as a distinct biofilm morphology that is functionally tied to surface-adhered biofilms and could serve as an antifungal- and immune-resistant dispersal mechanism.

INTRODUCTION

In natural and host environments microbes commonly grow in multicellular communities known as biofilms. Biofilms are physiologically and structurally complex cellular communities, embedded in a protective layer of extracellular material that provides a source of nutrients and protection against environmental stress and antimicrobial drugs (1). Depending on the environmental context, microbes can form functionally-distinct biofilm morphologies, varying by surface adhesiveness, species diversity, viability and internal architecture (2). Canonical microbial biofilms differentiate following attachment to biological or inert surfaces (3, 4). However, microbial biofilms can also occur in suspensions, forgoing the need for surface attachment. This is best described for bacterial biofilms that form independently of surface adhesion, for example in tissue fluid, thus defining surface-independent (aggregate) biofilms which are morphologically distinct from surface-adhered biofilms (5). These surface-independent bacterial biofilms are relevant in clinical, environmental and industrial settings, representing one of several nuances to biofilm development that led to a recent review highlighting the shortcomings of canonical models of bacterial biofilm formation that rely predominantly on studies of surface-adhered biofilms (5).

In addition to bacteria, yeasts are also prolific biofilm formers. A key example is the human yeast pathogen *Candida albicans*, for which biofilm formation is recognised as an important pathogenesis

mechanism (6–8). *C. albicans* biofilms affect mucosal sites of infection and medically implanted devices, including intravenous and urinary catheters, prosthetic joints and prosthetic heart valves (9). These biofilms add considerable treatment cost through prolonged hospitalisation and replacement of implanted devices (9). Biofilms worsen treatment outcomes through increased medical care needed to replace implanted devices (6, 7) and expose patients to a risk of systemic, high-mortality *C. albicans* infections in patients who are immunocompromised (6, 7, 10).

Despite the importance of biofilms in *C. albicans* disease, aspects of *C. albicans* biofilm development remain underexplored. As is the case for bacteria, mechanistic studies of *C. albicans* biofilms have focused predominantly on canonical, surface-adhered biofilms. The maturation of *C. albicans* biofilms is commonly described as a four-stage cycle: adherence, initiation, maturation and dispersal (8, 11). First, planktonic yeast cells adhere to a solid surface (adherence) before proliferation into an adhered, basal layer (initiation). Maturation is marked by the transition to filamentous cell morphologies and deposition of an extracellular matrix encasing a community of yeast, hyphal and pseudohyphal cells (8, 11). In the final, least studied of these biofilm stages, mature biofilms release yeast cells that establish growth at new sites (dispersal) (12, 13). An alternative to planktonic yeast cell dispersal has also been described, in which sections of mature, surface-adhered biofilms shear away under flow conditions, potentially seeding new biofilm growths elsewhere (14).

Biofilm differentiation is controlled by transcriptional programs, with six biofilm master transcription factors (TFs): Bcr1, Brg1, Efg1, Tec1, Ndt80 and Rob1 (15). These master regulators predominantly control two key aspects of biofilm formation: substrate and cell-cell adherence via adhesin gene expression, as well as filamentous morphogenesis (15). Additionally, the transcription factor Zap1 regulates extracellular matrix maturation in *C. albicans* biofilms (16), while yeast cell dispersal is regulated by the gene *PES1*, and also modulated by the activity of the transcriptional activator Ume6 (promotes filamentous morphology by activating the hyphal gene expression program) and the repressor Nrg1 (promotes yeast morphology by repressing the hyphal gene expression program) (12).

While extensively studied, the canonical surface-adhered biofilms of *C. albicans* may not represent the full spectrum of biofilm morphologies and functionalities that *C. albicans* can adopt for survival in the host. For example, *C. albicans* can form surface-adhered microcolonies (17) and suspended “mini biofilms” when co-cultured with the bacterium *Clostridium perfringens* (18). The mechanisms and functions of these, and any other non-canonical biofilm morphologies, are not well understood. Here we report an *C. albicans* biofilm morphology that is independent of surface adherence, that we named liquid-suspension biofilms. We provide a detailed characterisation of this biofilm morphology, including its functional connection to surface-adhered biofilms, potentially as an antifungal-resistant and stress-tolerant dispersal mechanism.

RESULTS

C. albicans forms structurally complex liquid-suspension biofilms in the absence of an adherence-permissive surface

Surface-adhered *C. albicans* biofilms can be cultured *in vitro* by seeding yeast cells onto a plastic surface in a conducive culture medium, for example MOPS-buffered RPMI, pH 7 (19). These yeast cells germinate into filamentous hyphal cells after adhering to the surface, followed by biofilm maturation (8, 11). *C. albicans* mutants with reduced adhesion are deficient in biofilm formation (20), and adhesion-resistant surfaces lead to decreased biofilm growth (21).

We attempted to reproduce this by culturing *C. albicans* biofilms on agarose surfaces (in liquid RPMI medium as above, SC5314 strain), predicting that poor adherence to the agarose surface would inhibit biofilm formation. Growth along the agarose surface was sparse compared to the plastic surface, but dense, irregular growths were observed in suspension (Fig. 1A). These growths were easily removed from wells by aspirating culture suspensions. To a lesser extent, similar suspension growths were observed for *C. albicans* biofilms cultured on plastic surfaces (Fig. 1A **and** Fig. 1B, right panel), although the extent of this growth varied between biological repeats. Suspended aggregate growths also formed in the presence of 10% Fetal Bovine Serum (FBS) and in filamentation-inducing Spider medium, tissue culture Dulbecco's Modified Eagle (DMEM) medium, as well as in rich YPD medium routinely used to culture fungi, although to a lesser extent (Fig. 1B, left panel).

To quantify suspended growths, we constructed an ImageJ, machine learning-based imaging analysis workflow to measure the total area of growth (Fig. 1C). This showed that *C. albicans* suspension growths are significantly larger in the presence of an agarose surface compared to a plastic surface (Fig. 1D). The imaging-based quantification was validated with XTT metabolic assays. With a plastic surface, surface growth was high and suspension growth was low at 5 and 24 hours post-seeding (Fig. 2A). In contrast, with an agarose surface, growth was higher in suspension than on the surface (Fig. 2B). The *rob1Δ/Δ* mutant, which lacks one of the master biofilm regulators, showed low surface and suspension growth in both plastic and agarose surface conditions, indicating that the suspension growth may be a form of biofilm growth (Fig. 2C).

To investigate the architecture of the suspension biofilms at the cellular level, we longitudinally sectioned formalin-fixed paraffin-embedded (FFPE) *C. albicans* liquid-suspension biofilms (Fig. 3A). This allowed for a depth-dependent (z-axis) view of *C. albicans* liquid-suspension biofilm structures. Periodic Acid-Schiff (PAS) staining showed a thick band of growth (~ 400–600 μm) with dense clusters of growth closer to the air-liquid interface (Fig. 3A). Specimens were prepared for confocal microscopy by staining cell walls (Concanavalin-A-488), intracellular protein (SYPRO Ruby) and nuclei (DAPI). This revealed that these dense clusters of growth were interconnected by a vast network of hyphae (Fig. 3B). Along the surface-liquid interface, growth was sparse (Fig. 3A, Fig. 3B), supporting a lack of surface growth for this culture condition (Fig. 2B). Yeast and hyphal cell morphologies were seen inside the dense cell clusters

near the air-liquid interface (Fig. 2B). Collectively, these findings show that *C. albicans* liquid-suspension growths are highly organised multicellular structures that are distinct from surface-adhered biofilms and planktonic growth.

Liquid-suspension biofilms share transcriptional regulation with surface-adhered biofilms

To further understand liquid-suspension biofilms, we performed RNAseq at early (5 h) and mature (24 h) timepoints, and compared them to canonical, surface-adhered biofilms (Fig. 4A). We also profiled planktonic *C. albicans* cultures grown for 3 h in the same (RPMI) medium as controls. Data analyses are presented in **Datasets S1** (gene expression, Venn diagram data) and **Dataset S2** (GO analysis results) and the data can be interactively explored using our Degust viewer (link).

Relative to planktonic cultures, both liquid-suspension and surface-adhered biofilms showed a pronounced transcriptional response at 5 h, which increased in mature biofilms at 24 h (Fig. 4B). Of the upregulated genes in liquid-suspension biofilms at 5 h, 59% were also upregulated in surface-adhered biofilms and the overlap increased to 69% at 24 h (Fig. 4C, **Dataset S1**). The overlap was smaller for the downregulated genes at 5 h (22%) but it similarly increased to 53% at 24 h (**Figure S1A**). GO analyses (Candida Genome Database GO term finder, REViGO tool to reduce redundancy) showed that genes upregulated relative to planktonic cells in both biofilm morphologies were enriched in functions required for cellular growth, translation, ribosome biogenesis, glycerol and amino acid metabolism, stress responses, iron transport and adhesion (**Figure S2A, Figure S3A, Dataset S2**). This is in line with robust biofilm proliferation. Genes downregulated in both biofilm morphologies were enriched for carbohydrate, nucleotide and amino acid metabolism and transport, particularly at 24 h (**Figure S2B, Figure S3B and Dataset S2**). This is consistent with nutrient depletion over time due to robust biofilm growth. Gene ontology terms related to cytoskeleton, filamentation and stress responses were also downregulated (**Figure S2B, Figure S3B, Dataset S2**), in line with a distinct morphology of both liquid-suspension and surface-adhered biofilm relative to planktonic cells.

At 5 hours, the cell wall adhesin *RBT1* (22) and the membrane lipid transporter *RTA3* (23) genes were upregulated in both biofilm morphologies: both with established roles in promoting biofilm formation (Fig. 4B, top panel) (24). *RTA3* is typically upregulated along with the transporters *CDR1* and *CDR2* in fluconazole-resistant clinical isolates (23). *CFL11* (FRE family member, NADPH oxidase gene), AAH1 (adenine deaminase gene) and PHO89 (inorganic phosphate transport gene) were also upregulated in both biofilm morphologies at 5 hours: indicating that both morphologies enter a multi-nutrient scavenging state in RPMI medium at an early stage (Fig. 4B, top panel). Two cell wall genes were prominently upregulated in liquid-suspension biofilms, but not in surface-adhered biofilms: *PGA31* and *YWP1* (Fig. 4B, top panel), which could be a consequence of the observed differences in biofilm architecture (Fig. 3). The Rbt5-family surface heme-binding protein *CSA2*, required for heme-iron catabolism (25), was amongst the mostly highly expressed genes in mature (24 h) liquid-suspension

biofilms (Fig. 4B, bottom panel). Other prominently upregulated genes in liquid-suspension biofilms were *INO1* (inositol biosynthesis), *PHO89* (inorganic phosphate transport), *RTA3* (membrane lipid translocation, roles in surface adhesion and azole resistance), *SAP4* and *SAP6* (aspartyl proteases) (Fig. 4B, bottom panel) (23, 26–30). Deletion of *CSA1*, *CSA2*, *PGA7*, *RBT5* and *SAP6* results in reduced *C. albicans* biofilm formation (28, 31–34). Along with *INO1*, *SAP4* and *PHO89*, these genes are all also upregulated in both liquid-suspension and surface-adhered biofilms at 24 h (Fig. 4B, bottom panel). The most prominently upregulated *C. albicans* liquid-suspension biofilm genes therefore have established roles in biofilm formation and are also upregulated in surface-adhered biofilms. Taken together, our RNAseq data shows that liquid-suspension biofilms largely share a transcriptional response with surface-adhered biofilms.

To identify differences between the two biofilm morphologies we performed pair-wise comparisons at both time points. At 5 h, 223 genes were differentially expressed at least 2-fold between liquid-suspension and surface-adhered biofilms, while at 24 h, 54 genes were differentially expressed between the two biofilm morphologies (**Dataset S1**). The bigger difference at 5 h likely reflects the different properties of the surface on which these biofilms were seeded (plastic versus agarose, i.e. high versus low adhesion). The comparison further shows that the two biofilm morphologies converge over the maturation time. GO analyses of genes differentially expressed in liquid-suspension biofilms relative to adhered biofilms showed that, at 5 hours, liquid-suspension biofilms prioritise cell proliferation more than surface-adhered biofilms and show reduced expression of metal transport and oxidative stress genes (Fig. 4D **and Dataset S2**). At 24 h, mature liquid-suspension biofilms show upregulation of genes involved in iron transport and homeostasis relative to surface-adhered biofilms, while they down-regulate some metabolic pathways, including iron-dependent processes such as cellular respiration and electron transport chain-related genes (Fig. 4D **and Dataset S2**). While iron-related genes are upregulated in mature (24 h) surface-adhered biofilms relative to planktonic controls, an even greater upregulation of iron genes is seen in mature (24 h) liquid-suspension biofilms (Fig. 4D, Fig. 4E). These changes are consistent with the Sef1-Sfu1-Hap43 circuit switching on during iron limitation: encoding a heme oxygenase (*HMX1*), ferric reductases (*FRE10*, *CFL1*), hemophores (*CSA1*, *CSA2*) and genes encoding FRE-family proteins that mediate heme uptake (*FRP1*, *FRP2*) (Fig. 4E).

This indicates that the iron starvation response is more prominently induced in mature liquid-suspension biofilms compared to surface-adhered biofilms. Iron chelation or supplementation (deferoxamine mesylate, ferric citrate) had no effect on *C. albicans* liquid-suspension biofilms morphologies (**Figure S4**) indicating that the iron response may be a consequence of liquid-suspension biofilm growth, rather than a strict requirement.

Master transcriptional regulators of surface-adhered biofilms also control C. albicans liquid-suspension biofilms

In *C. albicans*, six master transcription factors regulate surface-adhered biofilm formation: Bcr1, Brg1, Efg1, Ndt80, Rob1, Tec1 (15). To test their involvement in liquid-suspension biofilms, we cultured mutants for these biofilm master regulators, along with SN250 (parental lab strain) and SC5314 (clinical isolate from which the lab strain originated). An optimised liquid-suspension biofilm-generating agarose assay was used (Fig. 1A) followed by evaluation of suspension growth (Fig. 5A). The dense, punctate growths we had characterised for the liquid-suspension biofilms were absent in *rob1Δ/Δ* and *efg1Δ/Δ*, and less pronounced in *ndt80Δ/Δ*, *brg1Δ/Δ* and *tec1Δ/Δ* (Fig. 5A). Quantification using the XTT assay paralleled the morphology assessment and showed reduced liquid-suspension biofilms for *rob1Δ/Δ*, *efg1Δ/Δ*, *ndt80Δ/Δ* and *brg1Δ/Δ* (Fig. 5B). The ability of each mutant to form surface-adhered biofilm under our conditions (RPMI medium, pH 7, polystyrene plates) mirrored their ability to form *C. albicans* liquid-suspension biofilms (Fig. 5B). Although the *tec1Δ/Δ* mutant showed a degree of XTT-quantified growth that was comparable to the parental strain (Fig. 5B), the liquid-suspension morphology was clearly compromised based on microscopic data (Fig. 5A). The *bcr1Δ/Δ* mutant appeared to form normal *C. albicans* surface-adhered and liquid-suspension biofilms (Fig. 5A **& B**). This mirrors other reports that the *bcr1Δ/Δ* mutant forms normal surface-adhered biofilms in RPMI medium (35, 36).

Drug resistance and dispersal capabilities of C. albicans suspension biofilms

Antifungal resistance is a key functional trait of *C. albicans* surface-adhered biofilms (11). Sessile Minimum Inhibitory Concentration (SMIC50) assays showed that, like surface-adhered biofilms, liquid-suspension biofilms were resistant to the maximum concentration of fluconazole tested, while planktonic cells were susceptible (Table 1). Mirroring this, the efflux pumps *CDR1* and *MDR1* and membrane lipid transporter RTA3, associated with azole resistance, were upregulated in mature liquid-suspension biofilms and surface adhered biofilms (Fig. 4E)(23, 37). In contrast to fluconazole, *C. albicans* liquid-suspension biofilms were more sensitive to caspofungin compared to surface-adhered biofilms, with sensitivity similar to that of planktonic controls (Table 1).

Table 1
SMIC50 (sessile minimum inhibitory concentration) values of antifungals against surface-adhered and liquid-suspension biofilms.

Fluconazole		
Morphology	**SMIC50 (µg/mL, 95% CI)**	**R^2**
Surface-adhered biofilm	> 25	0.652
Liquid-suspension biofilm	> 25	0.595
Planktonic culture	0.322 (0.182–0.461)	0.977
Caspofungin		
Morphology	**SMIC50 (µg/mL, 95% CI)**	**R^2**
Surface-adhered biofilm	0.194 (0.069–0.320)	0.895
Liquid-suspension biofilm	0.072 (0.042–0.103)	0.983
Planktonic culture	0.068 (0.050–0.086)	0.986

Biofilms can disperse and seed infection at distal sites (12). Although robust *C. albicans* liquid-suspension biofilms formed when a poorly adhered surface (agarose) was present, we also observed dense, suspended growth in some mature, surface-adhered biofilms on plastic surfaces (Fig. 1B). We therefore hypothesised that *C. albicans* can transition between surface-adhered and liquid-suspension biofilms depending on surface availability, which may reduce when the surface is covered with the mature biofilm. This is supported by the overall transcriptomic profile of surface-adhered biofilms being more similar to that of liquid-suspension biofilms at 24 hours compared to 5 hours (r = 0.927 and r = 0.755, respectively, Fig. 6A). This observation suggests that *C. albicans* liquid-suspension biofilms might form after maturation of surface-adhered biofilms and aid in dispersal.

To test if *C. albicans* liquid-suspension biofilms could seed new surface-adhered biofilms, we transferred mature liquid-suspension biofilms (24 hours) to plastic surfaces and measured growth (XTT assay) along the surface after 5 hours (Fig. 6B). Supernatants were removed with P1000 pipette tips to ensure that all liquid-suspension biofilm growths were removed from wells, and three PBS rinses were performed before performing the XTT assay. This ensured that surface growth, not suspension growth, was quantified. Supernatants from *rob1Δ/Δ* mutants (biofilm-deficient control) were also transferred to plastic surfaces within these experiments and showed little to no surface growth. Liquid-suspension biofilm-seeded wells showed substantial growth along the surface, likely corresponding with early-stage surface adhered biofilm formation. Liquid-suspension biofilms derived from mature, surface-adhered biofilms at 48 hours were imaged, and the area of growth quantified (Fig. 6C, Fig. 6D). Importantly, the presence of suspended growths was confirmed with microscopy before collection (**Video S1**), and supernatants were carefully collected without dislodging surface-adhered biofilms. While not as

numerous as liquid-suspension biofilms observed in agarose surface conditions, liquid-suspension biofilms were isolated from surface-adhered biofilms cultured in RPMI and SPIDER media (Fig. 6C). While dense growths were observed in the suspensions of YPD-cultured biofilms, the high concentration of planktonic yeast cells made these harder to interpret as *C. albicans* liquid-suspension biofilms-like structures. Collectively, these data show that liquid-suspension biofilms form after the maturation of surface-adhered biofilms, and can seed new biofilm with fluconazole-resistant cells.

DISCUSSION

Here we show that *C. albicans* spontaneously forms liquid-suspension biofilms. This occurs in the absence of an adherent surface, such as in the liquid medium-agarose model that we established. It also occurs following maturation of a surface-adhered biofilm, whereby biofilm maturation exhausts available surface space triggering the transition from a surface-adhered to a liquid-suspension biofilm. The fact that a surface-adhered biofilm can produce liquid-suspension biofilms after maturation supports a functional relationship between these two biofilm morphologies. Most of our experiments used RPMI medium, but we confirmed that liquid-suspension biofilms form in a range of media conditions. Our data further shows that, as expected, with an adhesion-permissive surface *C. albicans* will preferentially form surface-adhered biofilms. However, lack of a strongly adherent surface does not prevent biofilm formation. Instead, it promotes the formation of liquid-suspension biofilms. This supports the idea that biofilms are the preferred growth morphotype for *C. albicans* under a range of physiological conditions, including within host tissues that resist surface biofilm establishment through adhesion-inhibiting mucin barriers and epithelial cell turnover (38).

In addition to being formed after full maturation of surface-adhered biofilms, we further show that liquid-suspension biofilms are azole resistant and can seed new biofilm growth, making them a potential vehicle for biofilm dispersal. Dispersal is the least-explored of the four stages of biofilm development (11). It has been predominantly characterized within the first 24 hours of biofilm growth, and defined as the release of planktonic yeast cells (13). Whether planktonic yeast cell release remains the dominant route for fully mature biofilms, particularly over longer, clinically-relevant timescales, warrants further investigation. Our findings show that the development of suspension biofilms from surface-adhered biofilms occurs at later stages of biofilm maturation, after 48 hours. Dispersing as an azole-resistant, multicellular suspended biofilm could provide a stress- and immune-resistant mechanism to disseminate, potentially affording more protection than dispersing as single yeast cells.

That the liquid-suspension biofilms are *bona fide* biofilms rather than simple aggregates is supported by our transcriptomics data, which shows that they largely share transcriptional regulation with surface-adhered biofilms, and are controlled by the same set of master transcriptional regulators. For example, already at 5 hours there is almost a 60% overlap between upregulated genes in liquid-suspension and surface-adhered biofilms, and by 24 hours the overlap is close to 70%. Moreover, several of the most strongly upregulated genes in liquid-suspension biofilms at 24 hours, including *CSA1*, *CSA2*, *PGA7*, *RBT5* and *SAP6*, have functionally validated roles in *C. albicans* surface-adhered biofilms (28, 31–34) and are

also upregulated in surface-adhered biofilms in our experiments (Fig. 4B). Of the biofilm master regulators, ROB1 and EFG1 are essential for the formation of liquid-suspension biofilms. NDT80, BRG1 and TEC1 are required but not essential, as mutants in these genes are able to grow some suspension biofilms, but with less biomass and/or with compromised morphology (Fig. 5B). Taken together, these findings show that liquid-suspension biofilms use the same regulatory networks as surface-adhered biofilms.

Despite similar transcriptional programs as surface-adhered biofilms, our confocal imaging showed that liquid-suspension biofilms are a distinct biofilm morphotype, characterised by dense growths of heterogenous *C. albicans* morphologies (yeast, pseudohyphae and hyphae) that are interconnected by vast hyphal networks (Fig. 3). This distinction is likely due to the difference in surface availability early in biofilm formation, during which surface-adhered biofilms normally adhere to a surface and proliferate. With a noticeable lack of surface adhesion, our imaging shows that *C. albicans* may be providing its own growing scaffold to adhere to within suspension (Fig. 3). *C. albicans* provides growth scaffolds for bacterial species in mix-culture biofilms (39), and similar scaffolding may seed and support the development of liquid-suspension biofilms. Moreover, mature liquid-suspension biofilms showed enrichment of iron acquisition and heme oxidation genes relative to surface-adhered biofilms, for example *HMX1*, *FRE10*, *CFL1*, *CSA1*, *CSA2*, *FRP1* and *FRP2*. There is very little iron in RPMI culture medium used in our study (which is not supplemented with iron), but FBS and ferric citrate-supplemented cultures showed no increase or decrease in the formation of liquid-suspension biofilms (**Figure S4**). *CSA1*, *CSA2* and *CFL1* have roles in cell differentiation and adhesion that promote biofilm formation: *csa1Δ/Δ* mutants have an aggregation defect (40), *csa2Δ/Δ* mutants show compromised yeast-to-hyphal switching and reduced biofilm formation (31), and *cfl1Δ/Δ* mutants show reduced adhesion to both abiotic surfaces and host epithelial cells (41). These phenotypes raise the possibility that the iron starvation response reinforces biofilm-favouring cell differentiation.

The globular liquid-suspension *C. albicans* biofilm morphologies we describe (Fig. 3) are distinct from the sheet-like structures of detached surface-attached biofilms, previously described as a distinct *C. albicans* dispersal process under flow conditions by Sellam et al. (14). Supporting this assertion, our liquid medium, agarose surface model shows that liquid-suspension biofilms form despite low surface growth, confirmed both by XTT metabolic assays and depth-dependent view confocal microscopy (Fig. 2, Fig. 3). These liquid-suspension biofilms are more similar to the suspended *C. albicans* growths termed “mini biofilms” induced upon co-culture with *C. perfringens*, described by Fox et al. (18), showing that suspension biofilms could be relevant for fungal-bacterial interactions.

Bacteria also form liquid-suspension biofilms and aggregates, which are relevant in several types of bacterial infections that establish in tissue fluids, as reviewed recently (2, 5). *C. albicans* liquid-suspension biofilms may similarly occur in clinical settings. Visible aggregates, ranging from solid clumps to smaller, “snowflake”-like growths have been described for *C. albicans* infection-affected patients with urinary catheters (42). These aggregates are typically a combination of *C. albicans* cells, epithelial cells and leukocytes (42). In cases of vulvovaginal candidiasis, which is predominantly caused

by *C. albicans*, a white, curd-like vaginal discharge is characteristic of infection (43), and microscopy of these growths show a combination of hyphae, pseudohyphae and leukocytes (44). Therefore, suspended host cells (epithelial cells and leukocytes) may offer *C. albicans* cells an adherence-permissive surface for suspended biofilm formation. In *C. albicans*-associated cases of candidemia, blood smears showing clusters of pseudohyphal cells are a common pathological feature (45, 46). More detailed microscopic analysis of blood, urine and vaginal discharge from *C. albicans*-affected patients would establish whether these suspended growths are a distinct liquid-suspension biofilm morphotype.

In conclusion, our study describes a liquid-suspension biofilm morphology for *C. albicans* that could aid in the dispersal of surface-adhered biofilms with antifungal-resistant cells. This provides a mode of dispersal that is additional to dispersing planktonic yeast cells. Understanding the roles of suspended biofilm morphologies in diseases is an exciting question for future studies.

MATERIALS AND METHODS

C. albicans strains, storage and culture

C. albicans strains used in this study, listed in **Table S1**, were maintained as glycerol stocks (15% glycerol) at -80°C. For reactivation, strains were streaked from frozen stocks onto YPD agar and incubated at 30°C for 2 to 3 days. YPD agar plates (1% yeast extract, 2% peptone, 2% glucose, 2% agar supplemented with 80 µg/mL uridine after autoclavation. Before seeding biofilms, single colonies were used to inoculate YPD liquid cultures which were then shaken at 200 rpm, 30°C for 16 to 20 hours.

Biofilm culture: surface-adhered and liquid-suspension biofilms

Unless otherwise stated, biofilm assays were performed in RPMI-1640 medium without phenol red (Sigma, #R8755) buffered with 165 mM MOPS and adjusted to pH 7.0 with sodium hydroxide, followed by membrane filtration (0.2 µm). Where indicated, RPMI-1640/MOPS was supplemented with 10% Fetal Bovine Serum (Bovogen Biologicals). Additional conditions tested were DMEM (Gibco #12100-061, supplemented with 3.7 g/L sodium bicarbonate and 0.11 g/L sodium pyruvate), Spider (1% Oxoid Nutrient Broth, 1% D-mannitol and 0.2% dipotassium phosphate supplemented with 80 µg/mL uridine after autoclavation) and YPD (as above).

For liquid-suspension biofilms, log-phase YPD cultures were diluted to OD_{600} 0.16 (an approximation of 3 x 10^6 cells/mL) into the relevant medium and seeded onto a surface of 2% low-melting-point (LMP) agarose (Bio-Rad, #1613111). For surface-adhered biofilms, the equivalent cell suspension was seeded directly onto an uncoated plastic well surface. Two plate formats were used depending on the downstream assay: 1) 24-well format (Fig. 1, 3, 5A, 6C, 6D, all microscopy %FOV data): 500 µL 2% LMP agarose per well (where applicable) and 500 µL of OD_{600} 0.16 cell suspension, 2) 96-well format (Fig. 2, 5B, 6B, all XTT assays): 100 µL 2% LMP agarose per well (where applicable) and 100 µL of OD_{600} 0.16 cell suspension. Plates were then incubated at 37°C with 60 rpm agitation for 90 min to allow for surface

adherence. Medium was then aspirated, wells were rinsed with sterile PBS, and fresh medium added, before returning plates to 37°C with 60 rpm agitation for a further 24 h (mature biofilm, 24 h). For the 48 h surface-adhered biofilm conditions (Fig. 6C, 6D), a second medium change was performed at 24 h without a PBS wash step, to avoid disturbing the mature biofilm, and plates returned to 37°C with 60 rpm agitation for a further 24 h.

XTT assays

Metabolic activity was assessed using the XTT Cell Proliferation Kit II (Sigma, #11465015001) as per manufacturer instructions. To distinguish between surface-adhered and suspension growth (Fig. 2), liquid medium with suspension growths was transferred to new wells before addition of XTT and phenazine methosulfate (PMS) mixture (two wells per growth condition). For all surface-adhered biofilm conditions (Figs. 2, 5 and 6), 100 µL of PBS was added to each well before XTT and PMS mixture was added. After the 37°C incubation step (30 minutes, no agitation), the XTT reaction mixture for surface-adhered biofilm or agarose layer conditions were transferred to new wells before absorbance reading (to avoid background absorbance from biofilm or agarose). Importantly, aspiration of liquid-suspension biofilms was done with P1000 pipette tips, as smaller tips failed to collect large, suspended growths. Absorbance was measured on a Tecan Spark 10M (SparkControl V2.3, firmware ABS V4.2.10) at 492 nm with a reference wavelength of 650 nm. Readings were background-corrected against media or PBS-only control wells. Statistical tests and data plotting was performed in R (v4.5.2) using ggplot2 (v4.0.3).

Dissection microscopy and FIJI/ImageJ quantification

Biofilms grown in the 24-well format (above) were imaged using an Olympus MVX10 dissection microscope at 4× magnification. Images were processed using the LabKit machine-learning segmentation plugin within FIJI/ImageJ (Fig. 1C). For each independent biological repeat, one image of liquid-suspension *C. albicans* biofilm was used to train a segmentation classifier, with suspended/surface growth labelled as foreground and empty well area and well-border shadow labelled as background and border, respectively. A batch macro applied this classifier to all images from the same biological repeat and exported a .csv file of foreground pixel area. False positives (for example, well-border artefacts) were identified by manually comparing input and output images and were corrected manually where necessary. Foreground area was expressed as % field-of-view (FOV) coverage. Statistical tests and data plotting was performed in R (v4.5.2) using ggplot2 (v4.0.3).

FFPE sectioning and confocal microscopy

Liquid-suspension biofilms were grown on a 2% LMP agarose surface (strain SC5314) in RPMI-1640/MOPS (pH 7.0) as described above. 500 µL of 2% LMP agarose (Bio-Rad), cooled to near 37°C, was gently added over the mature biofilm and incubated at 37°C for 1 h. The resulting agarose disc, containing the two agarose layers sandwiching the biofilm, was removed (room temperature) and trimmed to a 25×50 mm rectangle. This block was embedded within a further 2% LMP agarose pour in a plastic mould (150×150×50 mm), set for 30 min, and trimmed with approximately 10 mm of padding

around the encased sample. The trimmed block was placed between two biopsy pads in an FFPE cassette and fixed overnight in 10% neutral buffered formalin before paraffin processing, embedding, and sectioning by the Monash Histology Platform (MHP). Sections were cut at 5 µm onto Superfrost Plus slides (Thermo Scientific).

For overview imaging, adjacent serial sections from the same paraffin block were stained with Periodic Acid–Schiff (PAS) by MHP. For confocal imaging, sections were dewaxed by MHP, then permeabilised in PBS with 2% Triton X-100 for 1 h at room temperature. Slides were stained for 1 h at room temperature, protected from light, with Concanavalin A-FITC (1:200 dilution of 1 mg/mL stock, Sigma # C7642) and DAPI (1:1000 dilution, Sigma # D9541) diluted in PBS with 0.5% Triton X-100. After a PBS rinse, slides were again stained with SYPRO Ruby (1× working solution, Sigma # S4942) for a further 30 minutes, followed by another PBS rinse. Slides were then mounted using DAKO fluorescent mounting medium (Agilent, # S302380-2) under a 12 mm No. 1.5 coverslip, sealed with clear nail polish, and stored in the dark at room temperature overnight prior to imaging. Confocal imaging was performed on a Zeiss LSM 980 with Airyscan detector, using a C Plan-Apochromat 63×/1.40 oil-immersion objective. Images were acquired as tiled 512 × 512-pixel frames at 1.5× zoom with line averaging (2×) in unidirectional scan mode, at 16-bit depth, and stitched using ZEN's Stitch-and-Fuse algorithm.

RNA extraction, RNA sequencing and transcriptomics analysis

RNA sequencing was performed on the *C. albicans* strain SN425. YPD cultures, inoculated by single colonies, were grown for 17h at 30°C with 200 rpm agitation, before seeding of biofilms (OD_{600} 0.16) in RPMI-1640/MOPS. For early (5 h) biofilm samples, 20 mL of cell suspension was seeded onto agarose-layered (10mL of agarose per dish, liquid-suspension biofilms only) or uncoated (surface-adhered) petri dishes, incubated at 37°C with 60 rpm agitation (allowing adherence for 90 minutes), washed with PBS, and incubated at 37°C with 60 rpm agitation for a further 3 h, in 20 mL fresh RPMI-1640/MOPS. Surface and suspension growths were then pooled and harvested into 50 mL conical tubes (surface biofilms removed using cell scrapers, four tubes used per condition) and pelleted by centrifugation (3000 rpm, 5 min, room temperature). Then, 49 mL of supernatant was removed, and pellets resuspended in milliQ water before transfer to 1.5 mL screw-cap tubes. These suspensions were then re-pelleted (3000 rpm, 5 min, 4°C). Supernatants were discarded, and remaining pellets were snap-frozen on dry ice and stored at -20°C prior to extraction. For mature (24 h) biofilm samples, biofilms were grown in 6-well plates (600 µL 2% LMP agarose per well for liquid-suspension biofilms, no agarose for surface-adhered, seeding 1 mL of cell suspension per well) at 37°C with 60 rpm agitation. At 24 h, surface-adhered and liquid-suspension biofilms were removed (as described for 5 h biofilms above), and pooled into 50 mL tubes. Biofilms were then pelleted by centrifugation (3000 rpm, 5 min, room temperature), resuspended in 1 mL cold sterile milliQ water, transferred to screw-cap tubes, and re-pelleted (3000 rpm, 5 min, 4°C) before the supernatant was discarded and the pellet was snap-frozen on dry ice. For planktonic samples, overnight YPD cultures (as described for biofilm conditions) were diluted to OD_{600} 0.3 in RPMI-1640/MOPS, grown

for a further 3 h, then pelleted by centrifugation (3000 rpm, 5 min, room temperature), washed in cold sterile milliQ water, and re-pelleted (3000 rpm, 5 min, 4°C) before snap-freezing.

Thawed cell pellets were resuspended in 400 µL TES buffer, then lysed by the addition of 400 µL acidic phenol:chloroform for 1 h (5:1, 65°C, with vortexing every 15 min), followed by chloroform re-extraction, sodium acetate/ethanol precipitation, and resuspension in DEPC-treated water. Extracted RNA was treated with TURBO DNase (Invitrogen, #AM2238), followed by phenol:chloroform inactivation and ethanol wash. RNA quality and yield were assessed by Nanodrop spectrophotometry (NanoDrop 2000, Thermo Fisher Scientific USA) and 1% agarose gel electrophoresis.

Library preparation and RNA sequencing were performed using a NovaSeqX instrument with the Illumina DRAGEN BCL Convert pipeline, as previously described (47). The Tail Tools pipeline (version 1.9) was used to align reads to the genome and count UMIs (48). The reference genome used was *Candida albicans* SC5314 assembly 21, supplemented with the AF167163.1 locus. Differential expression analysis was performed in Degust (version 4.5) (49) using the limma-voom method (50), with genes considered significantly differentially expressed at FDR < 0.05 and $\log_2$ fold-change ≥ 1. A minimum CPM value of 5 in at least 4 samples were used as the cut-off. There was a batch effect for replicate 1 relative to replicates 2–4. Therefore, replicate 1 was used as a hidden factor in the analyses to correct for batch effects. Volcano plots were generated in R (v4.5.2) using EnhancedVolcano (v1.28.2). Diverging bar plots showing biofilm induced, biofilm repressed and “both” genes as a percentage of total gene number were generated in ggplot2 (v4.0.3). Gene Ontology (GO) term enrichment analysis was performed using the CGD GO Term Finder tool, with a background set of 6,672 genes, a p-value cutoff of 0.01, and Benjamini-Hochberg correction for multiple testing. GO term lists for each condition were plotted in R (v4.5.2) using CGD-exported TSV files alongside condensed REVIGO (51)- consolidated GO terms, used to reduce redundancy among enriched terms by semantic similarity clustering (dispensability threshold < 0.1, whole UniProt database background). Pearson correlation coefficients comparing $\log_2$ fold-change values between liquid-suspension and surface-adhered biofilms at each timepoint were computed in R across all detected genes.

Antifungal susceptibility testing (sessile minimum inhibitory concentration

Antifungal susceptibility assays of liquid-suspension and surface-adhered biofilms was based on standardised XTT-based biofilm susceptibility methods of Ramage et al. (52) and Pierce et al. (19). All assays used *C. albicans* SC5314. Biofilms were grown in the 96-well format described above for 24 h (100 µL per well). Fluconazole (Sigma-Aldrich, #F8929; dissolved in DMSO) and caspofungin (Sigma, #SML0425, dissolved in water) stocks (10 mg/mL) were diluted to top-well concentrations of 50 µg/mL (fluconazole) and 5 µg/mL (caspofungin) and serially diluted two-fold across the plate in RPMI-1640/MOPS. Antifungal dilutions were applied directly to 24 h-grown biofilms (100 µL solution per well, final well concentrations: fluconazole 25-0.049 µg/mL; caspofungin 2.5-0.0049 µg/mL). A 0.25% DMSO control (matching the DMSO concentration for the top fluconazole well) was included on each plate.

Planktonic controls were prepared fresh at OD_{600} 0.8 (from colony on YPD plate) and treated with the same antifungal dilution series and DMSO control in parallel. Plates were incubated stationary at 37°C for 24 h before metabolic activity was assessed by XTT assay as described above. Absorbance values were background-corrected against media-only control wells and expressed as percent viability relative to the DMSO vehicle-only control for each replicate. Dose-response curves were fitted in R using a four-parameter log-logistic model (drc package, LL.4 function) to the mean of % inhibition at each concentration. SMIC50 values (the antifungal concentration producing 50% inhibition of metabolic activity relative to the untreated control) were interpolated using the ED function with delta-method 95% confidence intervals, and goodness-of-fit was assessed by R^2 (1- SS_residual/SS_total) between fitted and observed mean inhibition values.

Declarations

DATA AVAILABILITY

Data generated in this study are provided within the manuscript and in the Supplementary Information. The transcriptomics data analyses (Datasets S1 and S2) and the numerical values from image-based quantification (field of view coverage) and XTT metabolic assay plots (Dataset S3) are provided in Supplementary Datasets S1, S2 and S3. Raw sequencing reads and processed gene counts have been deposited in the NCBI Gene Expression Omnibus under accession number GSE344593. The RNAseq data can also be explored interactively in Degust using this link. Raw microscopy images are available from Ana Traven (ana.traven@monash.edu) upon request.

ACKNOWLEDGMENTS

We thank Suzanne Noble and the Fungal Genetics Stock Centre for providing *C. albicans* SN strains and the Homann transcription factor mutant library from which the transcriptional regulator mutants were obtained (53, 54). We also acknowledge the infrastructure access and research support provided by the Monash MicroImaging Facility and Monash Genomics and Bioinformatics Platform. This work was supported by an Australian Research Council Discovery Project DP220102562 as well as Monash University strategic funds (to A.T.). A. T. is a National Health and Medical Research Council Investigator Fellow (ID 2033452).

AUTHOR CONTRIBUTIONS

F.A.B.O. and A.T. conceptualised the project and designed the study. F.A.B.O. and J.L.R. performed biofilm quantification, microscopy, imaging analysis and RNA extraction experiments. C.K-T, A.S., P.F.H. and T.H.B. performed and/or supervised library preparation, RNA sequencing and bioinformatic analyses. T.H.B. provided input into the RNAseq data interpretation. F.A.B.O., J.L.R. and P.F.H. performed RNAseq data analysis. A.T. supervised the project. F.A.B.O. was responsible for data visualisation and figure construction. F.A.B.O. and A.T. wrote the manuscript with input from co-authors.

References

1. Rather MA, Gupta K, Mandal M. Microbial biofilm: formation, architecture, antibiotic resistance, and control strategies. Brazilian Journal of Microbiology. 2021;52(4):1701–18.
2. Hall-Stoodley L, Costerton JW, Stoodley P. Bacterial biofilms: from the natural environment to infectious diseases. Nature Reviews Microbiology. 2004;2:95–108.
3. O'Toole G, Kaplan HB, Kolter R. Biofilm formation as microbial development. Annual Reviews in Microbiology. 2000;54(1):49–79.
4. Ramage G, Mowat E, Jones B, Williams C, Lopez-Ribot J. Our current understanding of fungal biofilms. Critical Reviews in Microbiology. 2009;35(4):340–55.
5. Sauer K, Stoodley P, Goeres DM, Hall-Stoodley L, Burmølle M, Stewart PS, et al. The biofilm life cycle: expanding the conceptual model of biofilm formation. Nature Reviews Microbiology. 2022;20(10):608–20.
6. Rajendran R, Sherry L, Nile CJ, Sherriff A, Johnson EM, Hanson MF, et al. Biofilm formation is a risk factor for mortality in patients with Candida albicans bloodstream infection—Scotland, 2012–2013. Clinical Microbiology and Infection. 2016;22(1):87–93.
7. Tumbarello M, Posteraro B, Trecarichi EM, Fiori B, Rossi M, Porta R, et al. Biofilm Production by Candida Species and Inadequate Antifungal Therapy as Predictors of Mortality for Patients with Candidemia. Journal of Clinical Microbiology. 2007;45(6):1843–50.
8. Nobile CJ, Johnson AD. Candida albicans Biofilms and Human Disease. Annual Review of Microbiology. 2015;69:71–92.
9. Ramage G, Martínez JP, López-Ribot JL. Candida biofilms on implanted biomaterials: a clinically significant problem. FEMS Yeast Research. 2006;6(7):979–86.
10. Pappas PG, Lionakis MS, Arendrup MC, Ostrosky-Zeichner L, Kullberg BJ. Invasive candidiasis. Nature Reviews Disease Primers. 2018;4:18026.
11. Gulati M, Nobile CJ. Candida albicans biofilms: development, regulation, and molecular mechanisms. Microbes and Infection. 2016;18(5):310–21.
12. Uppuluri P, Acosta Zaldívar M, Anderson MZ, Dunn MJ, Berman J, Lopez Ribot JL, et al. Candida albicans dispersed cells are developmentally distinct from biofilm and planktonic cells. mBio. 2018;9(4):e01338-18.
13. Uppuluri P, Chaturvedi AK, Srinivasan A, Banerjee M, Ramasubramaniam AK, Köhler JR, et al. Dispersion as an important step in the Candida albicans biofilm developmental cycle. PLoS Pathogens. 2010;6(3):e1000828.
14. Sellam A, Al-Niemi T, McInnerney K, Brumfield S, Nantel A, Suci PA. A Candida albicans early stage biofilm detachment event in rich medium. BMC Microbiology. 2009;9(1):25.
15. Nobile CJ, Fox EP, Nett JE, Sorrells TR, Mitrovich QM, Hernday AD, et al. A recently evolved transcriptional network controls biofilm development in Candida albicans. Cell. 2012;148(1–2):126–38.

16. Nobile CJ, Nett JE, Hernday AD, Homann OR, Deneault JS, Nantel A, et al. Biofilm Matrix Regulation by Candida albicans Zap1. PLoS Biology. 2009;7(6):e1000133.
17. McCall AD, Kumar R, Edgerton M. Candida albicans Sfl1/Sfl2 regulatory network drives the formation of pathogenic microcolonies. PLoS Pathogens. 2018;14(9):e1007316.
18. Fox EP, Cowley ES, Nobile CJ, Hartooni N, Newman DK, Johnson AD. Anaerobic bacteria grow within Candida albicans biofilms and induce biofilm formation in suspension cultures. Current Biology. 2014;24(20):2411–6.
19. Pierce CG, Uppuluri P, Tristan AR, Wormley FL, Mowat E, Ramage G, et al. A simple and reproducible 96-well plate-based method for the formation of fungal biofilms and its application to antifungal susceptibility testing. Nature Protocols. 2008;3(9):1494–500.
20. McCall AD, Pathirana RU, Prabhakar A, Cullen PJ, Edgerton M. Candida albicans biofilm development is governed by cooperative attachment and adhesion maintenance proteins. npj Biofilms and Microbiomes. 2019;5:21.
21. Chandra J, Patel JD, Li J, Zhou G, Mukherjee PK, McCormick TS, et al. Modification of surface properties of biomaterials influences the ability of Candida albicans to form biofilms. Applied and Environmental Microbiology. 2005;71(12):8795–801.
22. Braun BR, Head WS, Wang MX, Johnson AD. Identification and characterization of TUP1-regulated genes in Candida albicans. Genetics. 2000;156(1):31–44.
23. Whaley SG, Tsao S, Weber S, Zhang Q, Barker KS, Raymond M, et al. The RTA3 Gene, Encoding a Putative Lipid Translocase, Influences the Susceptibility of Candida albicans to Fluconazole. Antimicrobial Agents and Chemotherapy. 2016;60(10):6060–6.
24. Monniot C, Boisramé A, Da Costa G, Chauvel M, Sautour M, Bougnoux ME, et al. Rbt1 Protein Domains Analysis in Candida albicans Brings Insights into Hyphal Surface Modifications and Rbt1 Potential Role during Adhesion and Biofilm Formation. PLOS ONE. 2013;8(12):e82395.
25. Okamoto-Shibayama K, Kikuchi Y, Kokubu E, Sato Y, Ishihara K. Csa2, a member of the Rbt5 protein family, is involved in the utilization of iron from human hemoglobin during Candida albicans hyphal growth. FEMS Yeast Research. 2014;14(4):674–7.
26. Klig LS, Zobel PA, Devry CG, Losberger C. Comparison of INO1 gene sequences and products in Candida albicans and Saccharomyces cerevisiae. Yeast. 1994;10(6):789–800.
27. Acosta-Zaldívar M, Qi W, Mishra A, Roy U, King WR, Li Y, et al. Candida albicans' inorganic phosphate transport and evolutionary adaptation to phosphate scarcity. PLoS Genetics. 2024;20(8):e1011156.
28. Srivastava A, Sircaik S, Husain F, Thomas E, Ror S, Rastogi S, et al. Distinct roles of the 7-transmembrane receptor protein Rta3 in regulating the asymmetric distribution of phosphatidylcholine across the plasma membrane and biofilm formation in Candida albicans. Cellular Microbiology. 2017;19(12):e12767.
29. Miyasaki SH, White TC, Agabian N. A fourth secreted aspartyl proteinase gene (SAP4) and a CARE2 repetitive element are located upstream of the SAP1 gene in Candida albicans. Journal of Bacteriology. 1994;176(6):1702–10.

30. Buu LM, Chen YC. Sap6, a secreted aspartyl proteinase, participates in maintenance the cell surface integrity of Candida albicans. Journal of Biomedical Science. 2013;20(1):101.
31. Okamoto-Shibayama K, Kikuchi Y, Kokubu E, Sato Y, Ishihara K. Possible Involvement of Surface Antigen Protein 2 in the Morphological Transition and Biofilm Formation of Candida albicans. Medical Mycology Journal. 2017;58(4).
32. Winter MB, Salcedo EC, Lohse MB, Hartooni N, Gulati M, Sanchez H, et al. Global Identification of Biofilm-Specific Proteolysis in Candida albicans. mBio. 2016;7(5):e01514-16.
33. Srikantha T, Daniels KJ, Pujol C, Kim E, Soll DR. Identification of genes upregulated by the transcription factor Bcr1 that are involved in impermeability, impenetrability, and drug resistance of Candida albicans a/α biofilms. Eukaryotic Cell. 2013;12(6):875–88.
34. Pérez A, Pedrós B, Murgui A, Casanova M, López-Ribot JL, Martínez JP. Biofilm formation by Candida albicans mutants for genes coding fungal proteins exhibiting the eight-cysteine-containing CFEM domain. FEMS Yeast Research. 2006;6(7):1074–84.
35. Goerlich K, Solis NV, Filler SG, Mitchell AP. Shared antibiofilm targets of biofilm regulators Wor3 and Bcr1 in Candida albicans. Genetics. 2026;233(3):iyag129.
36. Huang MY, Woolford CA, May G, McManus CJ, Mitchell AP. Circuit diversification in a biofilm regulatory network. PLoS Pathogens. 2019;15(5):e1007787.
37. Ramage G, Bachmann S, Patterson TF, Wickes BL, López-Ribot JL. Investigation of multidrug efflux pumps in relation to fluconazole resistance in Candida albicans biofilms. Journal of Antimicrobial Chemotherapy. 2002;49(6):973–80.
38. Kavanaugh NL, Zhang AQ, Nobile CJ, Johnson AD, Ribbeck K. Mucins suppress virulence traits of Candida albicans. mBio. 2014;5(6):e01911-14.
39. Ponde NO, Lortal L, Ramage G, Naglik JR, Richardson JP. Candida albicans biofilms and polymicrobial interactions. Critical Reviews in Microbiology. 2021;47(1):91–111.
40. Kumar R, Breindel C, Saraswat D, Cullen PJ, Edgerton M. Candida albicans Sap6 amyloid regions function in cellular aggregation and zinc binding, and contribute to zinc acquisition. Scientific Reports. 2017;7:2908.
41. Yu Q, Dong Y, Xu N, Qian K, Chen Y, Zhang B, et al. A novel role of the ferric reductase Cfl1 in cell wall integrity, mitochondrial function, and invasion to host cells in Candida albicans. FEMS Yeast Research. 2014;14(7):1037–47.
42. Steixner S, Bauer A, Bellmann-Weiler R, Lass-Flörl C. Catheter-Associated Candiduria: Aggregates, Microscopy, and CFU Variability. Mycopathologia. 2026;191(2):40.
43. Rafat Z, Alipour N, Esmaeili E, Mirhasani F, Yaseri M, Haghighat F, et al. Vulvovaginal candidiasis: A global perspective through systematic review and meta-analysis. Microbial Pathogenesis. 2026:108284.
44. Agoni L. Old but gold: an historical perspective of wet mount microscopy and its current role for the diagnosis of vaginitis. Frontiers in Reproductive Health. 2026;8:1755906.

45. Harrington A, McCourtney K, Nowowiejski D, Limaye A. Differentiation of Candida albicans from non-albicans yeast directly from blood cultures by Gram stain morphology. European Journal of Clinical Microbiology & Infectious Diseases. 2007;26(5):325–9.
46. Park BRG, Kim T-H, Kim HR, Lee M-K. Comparative analysis of simulated candidemia using two different blood culture systems and the rapid identification of Candida albicans. Annals of Clinical & Laboratory Science. 2011;41(3):251–6.
47. Tedja I, Weerasinghe H, Bryak G, Stölting H, Lo TL, Simm C, et al. Candida auris uses nutrient sensing to modulate virulence and host immune responses. Nature Microbiology. 2026:1–16.
48. Harrison PF, Powell DR, Clancy JL, Preiss T, Boag PR, Traven A, et al. PAT-seq: a method to study the integration of 3'-UTR dynamics with gene expression in the eukaryotic transcriptome. RNA. 2015;21(8):1502–10.
49. Powell DR. Degust 4.5. Zenodo; 2019.
50. Law CW, Chen Y, Shi W, Smyth GK. voom: Precision weights unlock linear model analysis tools for RNA-seq read counts. Genome Biology. 2014;15(2):R29.
51. Supek F, Bošnjak M, Škunca N, Šmuc T. REVIGO Summarizes and Visualizes Long Lists of Gene Ontology Terms. PLoS ONE. 2011;6(7):e21800.
52. Ramage G, Vande Walle K, Wickes BL, López-Ribot JL. Standardized method for in vitro antifungal susceptibility testing of Candida albicans biofilms. Antimicrobial Agents and Chemotherapy. 2001;45(9):2475–9.
53. Homann OR, Dea J, Noble SM, Johnson AD. A phenotypic profile of the Candida albicans regulatory network. PLoS Genetics. 2009;5(12):e1000783.
54. McCluskey K, Wiest A, Plamann M. The Fungal Genetics Stock Center: a repository for 50 years of fungal genetics research. Journal of Biosciences. 2010;35(1):119–26.

Figures

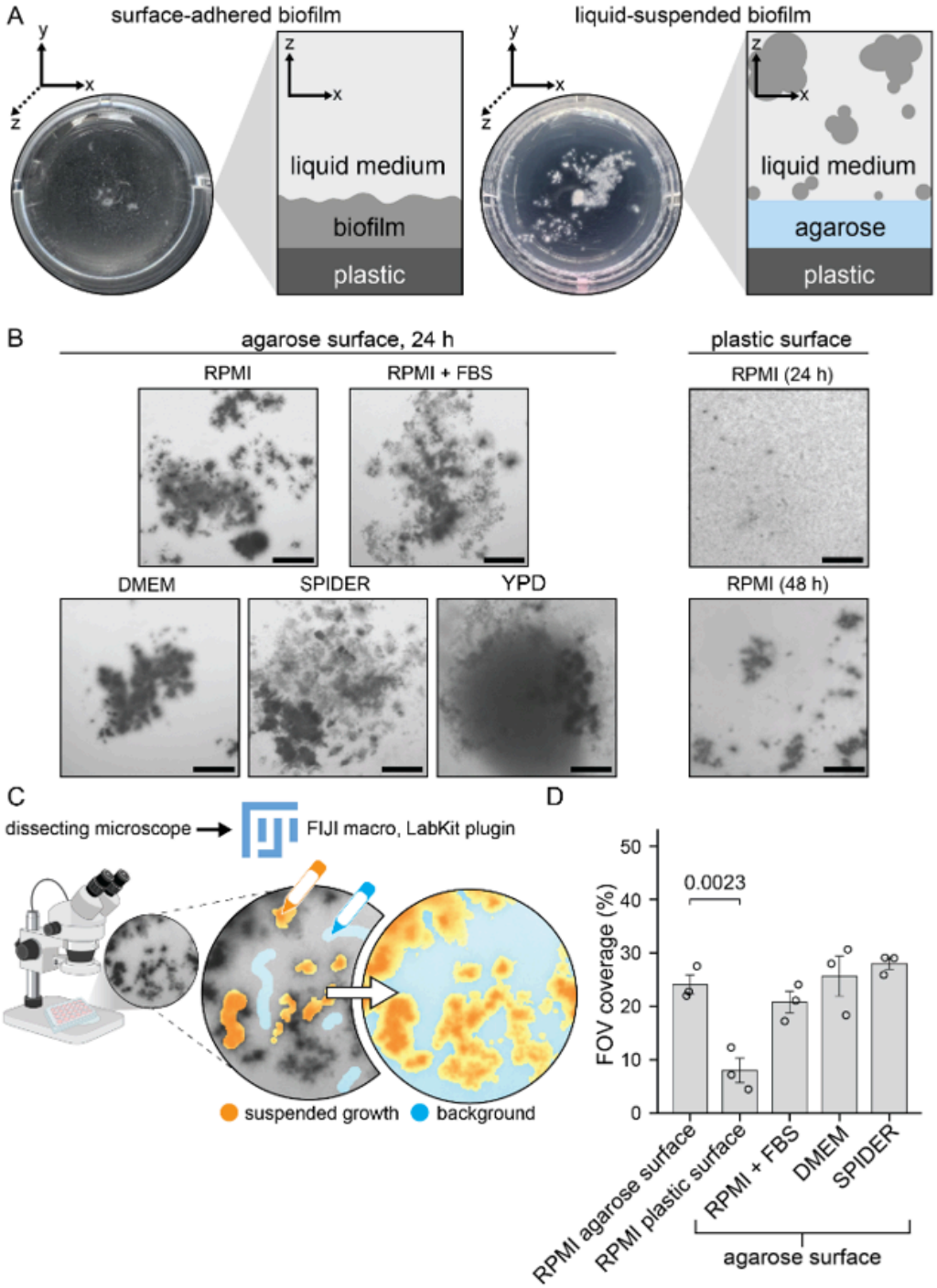


Figure 1

C. albicans forms suspended aggregates in liquid medium when faced with low- adherence surfaces.

a. Schematic and representative images of surface-adhered and suspension biofilms (24 hours). Compared to surface-adhered biofilms on plastic, a lack of surface-associated growth along agarose surfaces is accompanied by aggregates forming in suspension.

b. Microscopy images of suspended aggregates formed in liquid suspension with agarose surfaces (left) or plastic surfaces following the formation of a mature surface-adhered biofilm at 48 hours (right). Scale bar = 1.5mm.

c. Machine learning-based classification of growth in suspension (Labkit, ImageJ), used to calculate the total area of suspended growth in microscopy images.

d. Image-based quantification of suspension growth for conditions in panel B (one-way ANOVA with Dunnett's post hoc test, $p = 0.0023$, non-significant p-values not displayed). Shown are averages and the standard error of the mean (SEM) of 3 independent repeats. FOV (field of view) coverage: the total 2D area within the image field of view occupied by suspension growth.

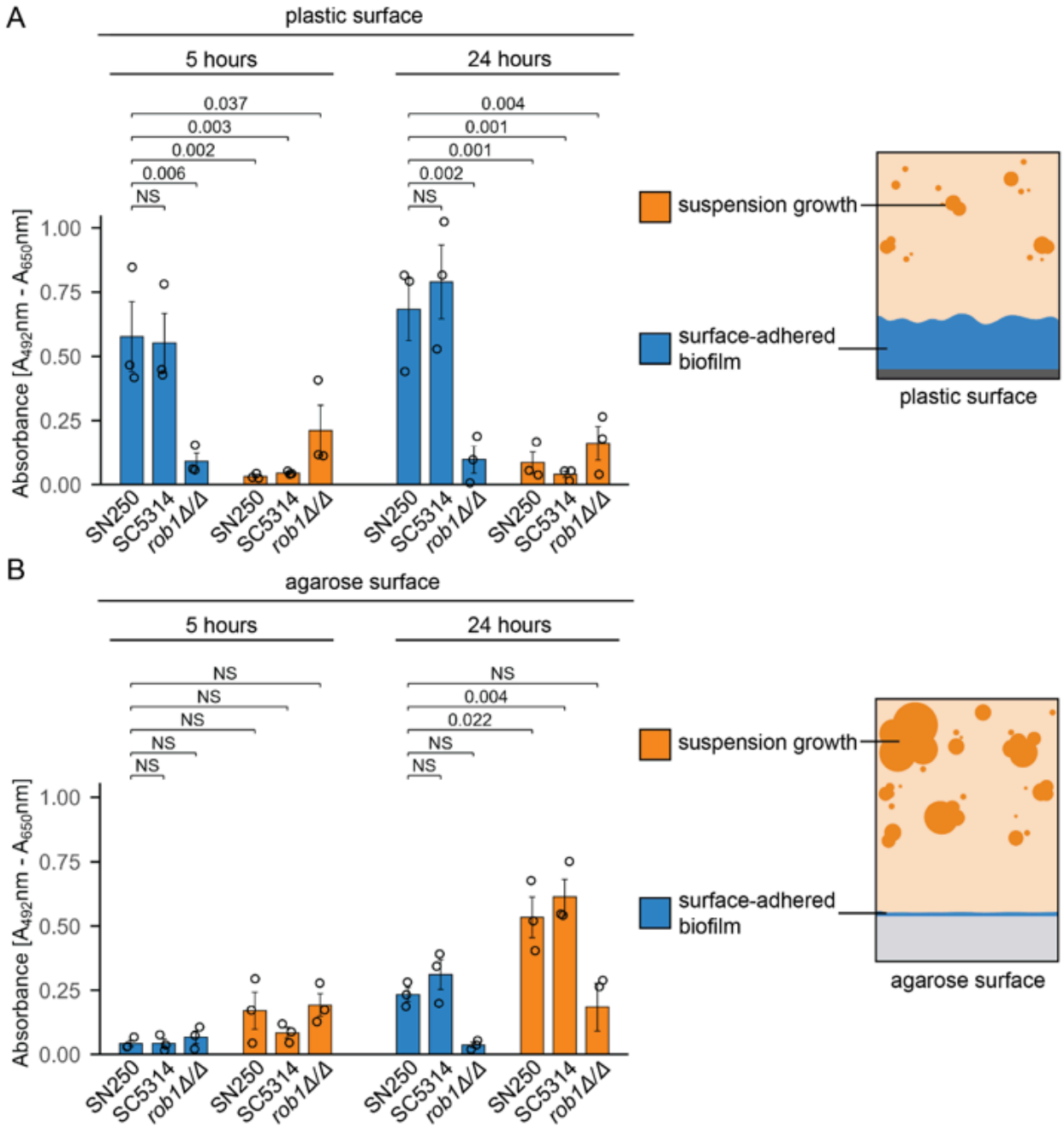


Figure 2

C. albicans suspension growth is enhanced on an agarose surface compared to a plastic surface.

a. XTT assay quantifying surface biofilm (blue) and suspension (orange) growth on plastic surfaces, at 5 hours and 24 hours post-seeding. The wild type strains were the clinical isolate SC5314 and the lab-strain SN250. The rob1Δ/Δ mutant was used a control, biofilm-defective strain. A one-way ANOVA with Dunnett's post hoc test was performed using SN250 surface biofilm growth as control (p-values displayed). Shown are averages and the SEM, n=3. NS- not significant.

b. As in A, but for agarose surfaces.

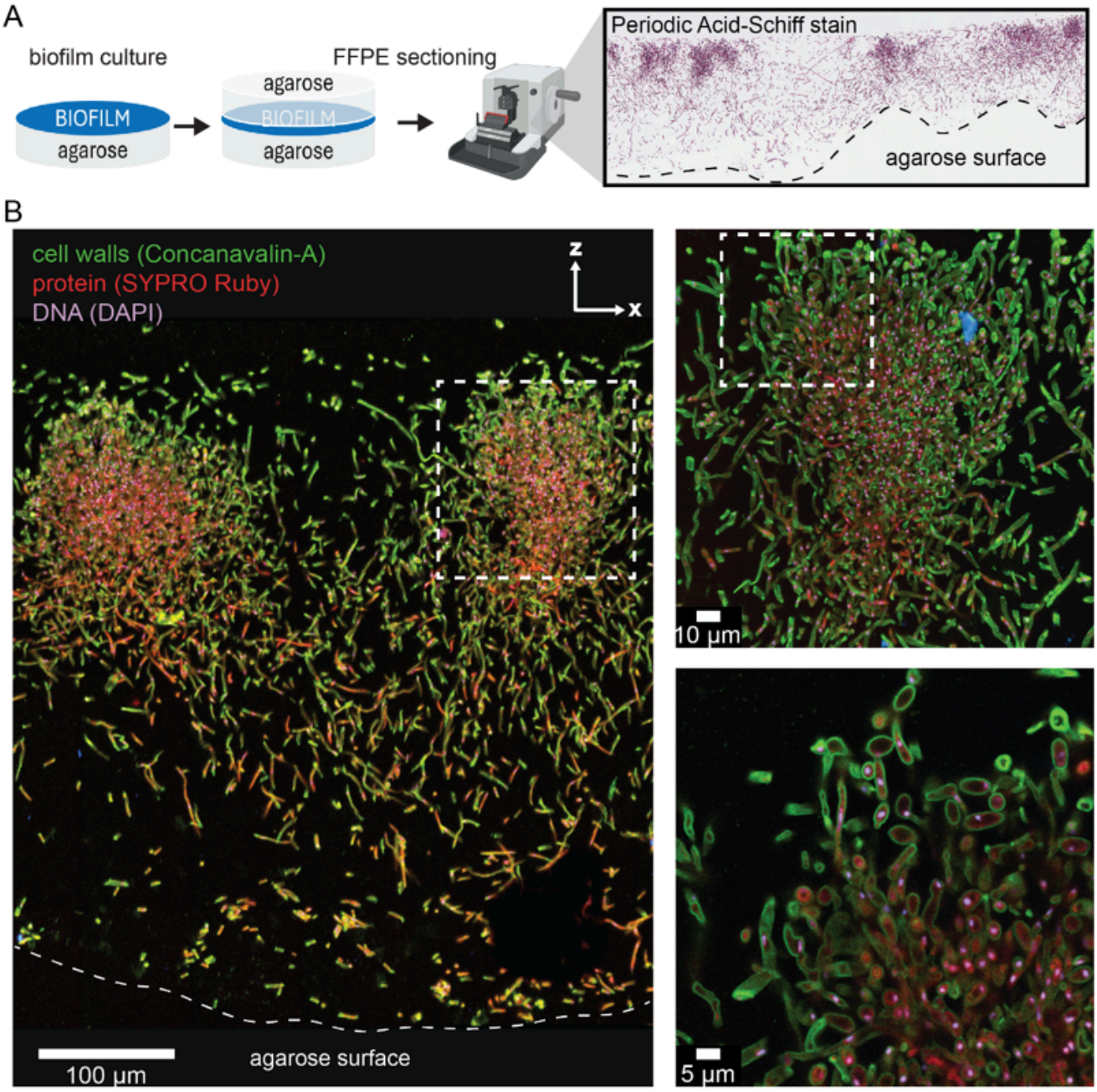


Figure 3

The architecture of *C. albicans*liquid-suspension biofilms.

a. C. albicans liquid-suspension biofilms were formalin-fixed and paraffin-embedded (FFPE) before microtome slicing along the z-axis, to provide a depth-dependent view of biofilm architecture. Biofilm architecture was visualised with PAS (Periodic Acid-Schiff) staining. Dotted line indicates the agarose surface.

b. Confocal microscopy of FFPE sections stained for cell walls (Concanavalin-A-488), intracellular protein (SYPRO Ruby) and nuclei (DAPI). Dotted line indicates the agarose surface.

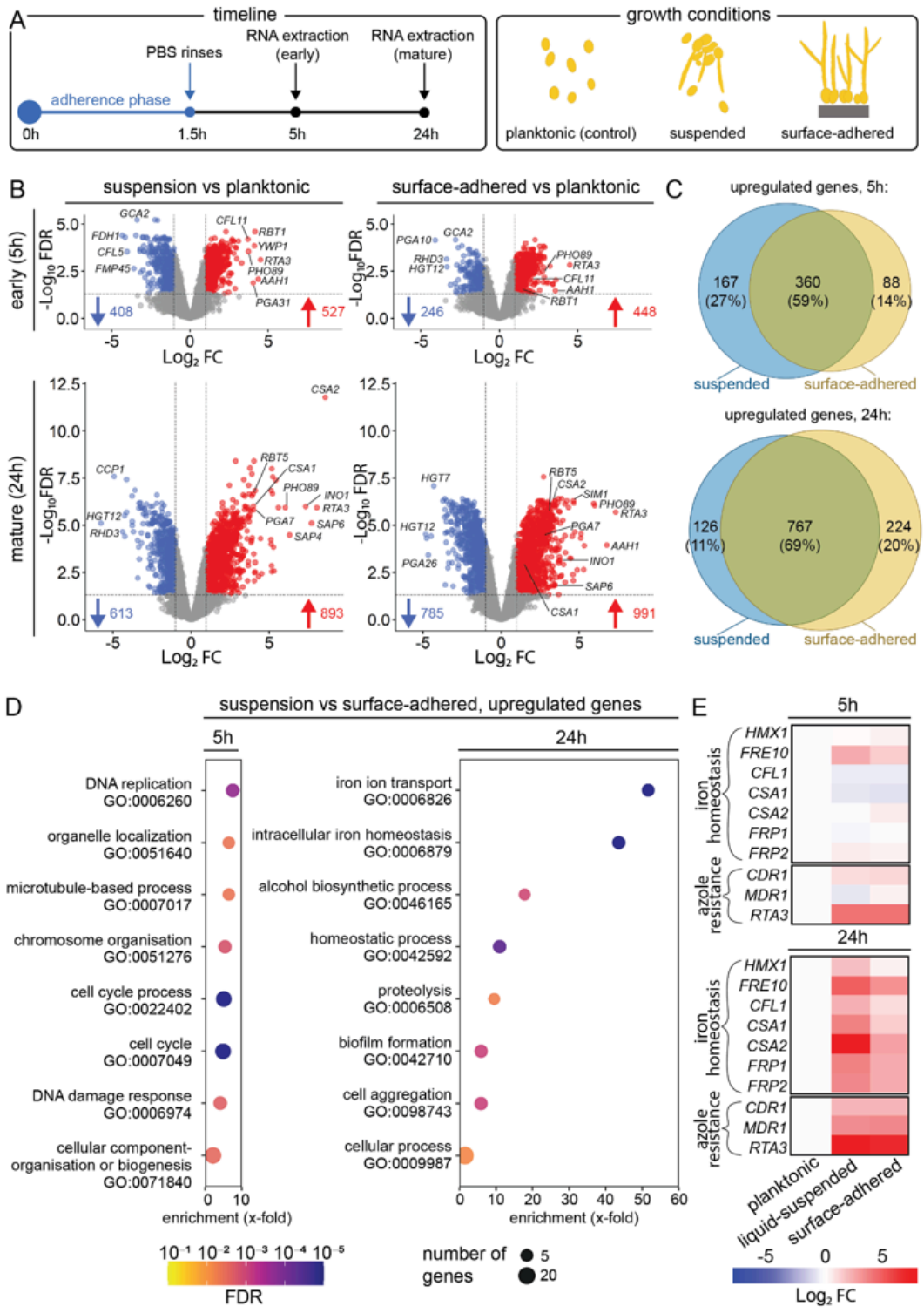


Figure 4

Liquid-suspension biofilms share transcriptional regulation with surface-adhered biofilms.

a. Overview of sample conditions: *C. albicans* liquid-suspension biofilms, surface-adhered biofilms sampled at early (5 hours) and mature (24 hours) time points and a planktonic control (3 hours).

b. Volcano plots of *C. albicans* liquid-suspension biofilms and surface-adhered biofilm gene expression changes compared to planktonic controls, at 5 (top panel) and 24 (bottom panel) hours. The horizontal line indicates the cut-off of Log_{10} FDR of 0.05 and the vertical lines indicates Log_2FC of 1. Upregulated genes are labelled in red, while downregulated genes are labelled in blue.

c. Venn diagrams showing the overlap in genes upregulated in liquid-suspension and surface-adhered biofilms at 5 and 24 hours.

d. Gene Ontology (GO) Analysis of genes upregulated in liquid-suspension biofilms relative to surface-adhered biofilms. The size of datapoints indicates number of genes assigned to a GO term, colour shows p-value.

e. Heatmaps of Log_2FC values for genes associated with iron homeostasis and azole resistance, normalised to planktonic conditions.

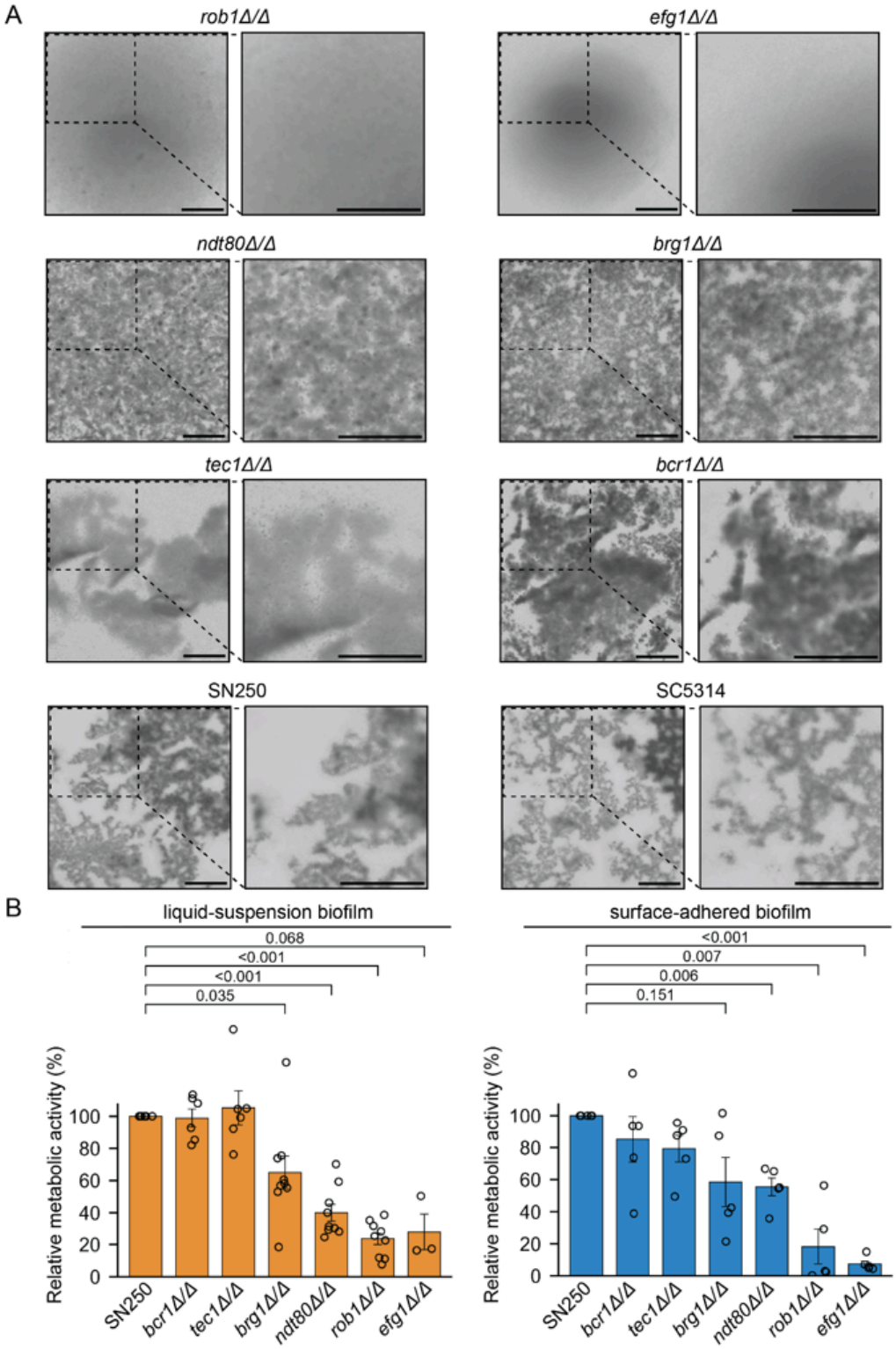


Figure 5

Master transcriptional regulators of surface-adhered biofilms also regulated liquid-suspension biofilms.

a. Suspension growth morphologies of the indicated mutants along with SN250 and SC5314 controls, cultured in RPMI + MOPS pH 7. Scale bar = 1.5mm.

b. XTT assay of liquid-suspension and surface-adhered biofilms formed by the indicated strains. Averages and SEM of n= 3-9 biological repeats (One-sample t-tests against a theoretical mean of 100% (representing the SN250 control), with Holm-Šídák correction for multiple comparisons).

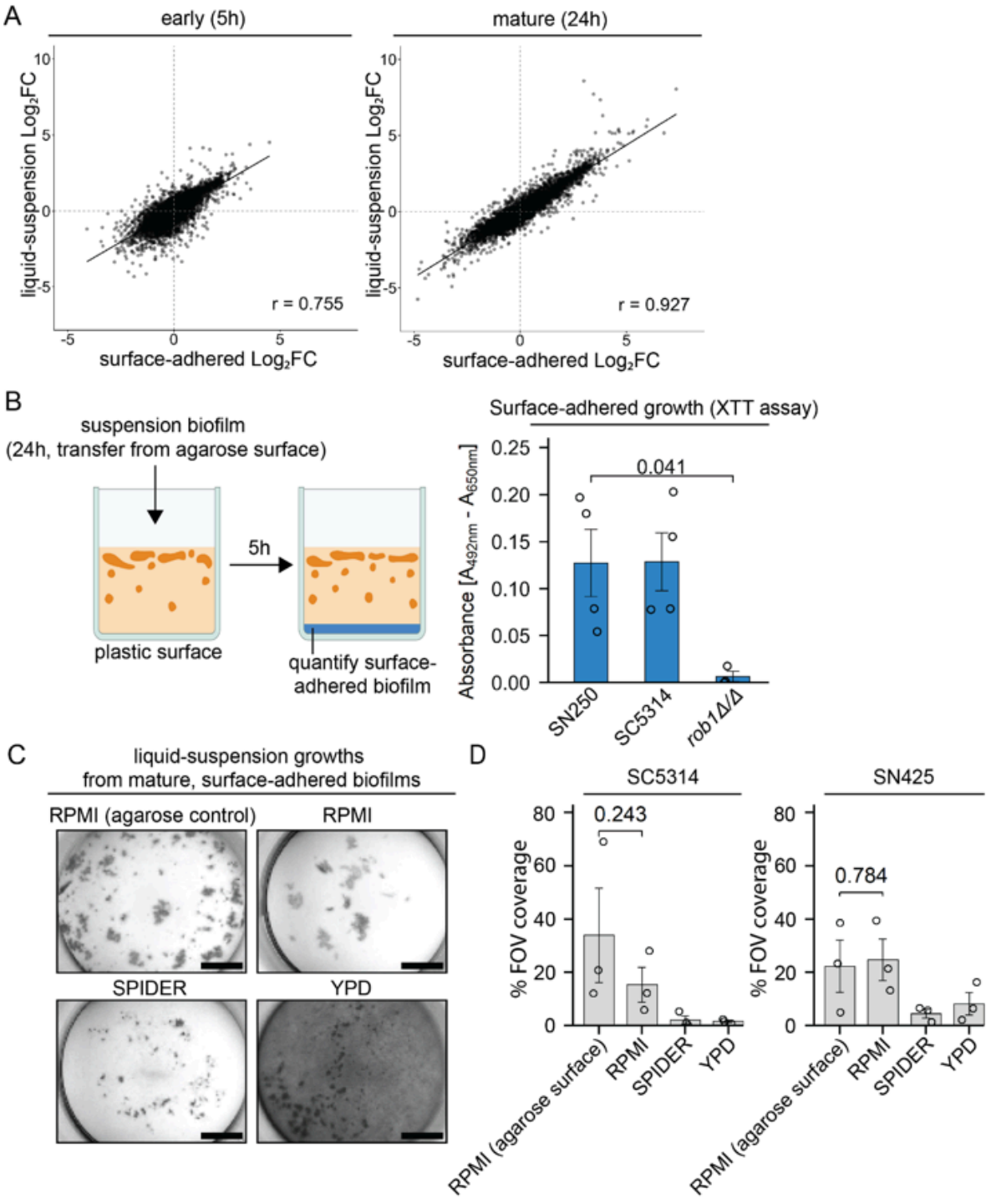


Figure 6

Surface-dependent interchange between surface-adhered and C. albicans liquid-suspension biofilms may promote biofilm dispersal and seeding.

a. Correlation plot of the transcriptomes of liquid-suspension biofilms and surface-adhered biofilms at 5 and 24 hours. Pearson's coefficients for each plot is shown.

b. XTT assay quantifying surface biofilm growth following transfer of liquid-suspension biofilms to a plastic surface. The rob1Δ/Δ mutant was used as a biofilm-negative control. Shown is the average of four (SN250, SC5314) or three (rob1Δ/Δ) repeats, error bars represent the SEM and the p-value displayed is that of a Welch's t-test comparison of rob1Δ/Δ to SN250.

c. Microscopy images of liquid-suspension biofilms grown from mature, surface-adhered biofilms. Scale bar = 3mm.

d. Imaging-based quantification of suspension growths originating from mature (48 hours) surface-adhered C. albicans biofilms. FOV (field of view) coverage: the total 2D area within the image field of view occupied by suspension growth. Three independent repeats are shown for each condition, with error bars representing the SEM. Paired t-tests performed comparing RPMI growths and that of RPMI with agarose surfaces, serving as s control for RPMI growths only (SPIDER, YPD agarose surface condition controls were not performed).

Supplementary Files

This is a list of supplementary files associated with this preprint. Click to download.

- OlivieretalSupplementaryFiguresandTablesLSbiofilms28092026.docx
- OlivieretalLSBiofilmDatasetS3280926.xlsx
- OlivieretalLSBiofilmDatasetS2280926.xlsx
- OlivieretalLSBiofilmDatasetS1280926.xlsx
- VideoS1.mp4